Biodegradation **9:** 1–10, 1998.

The role of biomineralization in microbiologically influenced corrosion *

Brenda Little[1,*], Patricia Wagner[1], Kevin Hart[1], Richard Ray[1], Dennis Lavoie[1], Kenneth Nealson[2] & Carmen Aguilar[2]
[1] *Naval Research Laboratory, Code 7333, Stennis Space Center, MS 39529, USA;* [2] *Center for Great Lakes Studies, University of Wisconsin, Milwaukee, WI 53204, USA (*author for correspondence)*

Accepted 24 July 1997

Key words: biomineralization, ferrihydrite, goethite, hematite, metal-reducing bacteria, microbiologically influenced corrosion, *Shewanella putrefaciens*

Abstract

Synthetic iron oxides (goethite, α-FeO·OH; hematite, Fe_2O_3; and ferrihydrite, $Fe(OH)_3$) were used as model compounds to simulate the mineralogy of surface films on carbon steel. Dissolution of these oxides exposed to pure cultures of the metal-reducing bacterium, *Shewanella putrefaciens*, was followed by direct atomic absorption spectroscopy measurement of ferrous iron coupled with microscopic analyses using confocal laser scanning and environmental scanning electron microscopies. During an 8-day exposure the organism colonized mineral surfaces and reduced solid ferric oxides to soluble ferrous ions. Elemental composition, as monitored by energy dispersive x-ray spectroscopy, indicated mineral replacement reactions with both ferrihydrite and goethite as iron reduction occurred. When carbon steel electrodes were exposed to *S. putrefaciens*, microbiologically influenced corrosion was demonstrated electrochemically and microscopically.

Abbreviations: CLSM – Confocal laser scanning microscopy; EDS – Energy dispersive x-ray spectroscopy; ESEM – Environmental scanning electron microscopy; MIC – Microbiologically influenced corrosion; SRB – Sulfate-reducing bacteria

Introduction

It has been established that the most devastating microbiologically influenced corrosion (MIC) takes place in the presence of microbial consortia in which many physiological types of bacteria interact in complex ways (Little et al. 1991a; Pope et al. 1984). However, many of the organisms in these consortia have yet to be characterized and the nature of the complex interactions remain uncharacterized. The groups of organisms that are most often cited as causative are the sulfate-reducing bacteria (SRB) and metal-depositing bacteria. SRB produce sulfide, initiating a variety of corrosive reactions, while metal-depositing bacteria produce visible tubercles (manganese and/or iron oxides) that are unmistakable in their appearance. SRB are ubiquitous and easily cultured and quantified. Several diagnostic kits have been developed for SRB based on sulfide reactions with metals (American Petroleum Institute 1965; Bioindustrial Technologies, Georgetown, TX) or the presence of specific enzymes, such as hydrogenases (Boivin et al. 1990) or reductases (Tatnall et al. 1988). Mineralogical fingerprints have been identified for corrosion processes induced by SRB on copper and ferrous substrata (McNeil & Little 1990, McNeil et al. 1991). A group of organisms about which much less is known in terms of role(s) in corrosion are the dissimilatory metal reducers. Dissimilatory iron and/or manganese reduction occurs in several microorganisms, including anaerobic and facultative aerobic bacteria. Inhibitor and competition experiments suggest that Mn(IV) and Fe(III) are efficient electron acceptors similar to nitrate in redox ability and are capable of out-competing electron acceptors of lower potential, such as sulfate or

carbon dioxide (Myers & Nealson 1988). Many of the recently described metal reducers are capable of using a variety of electron acceptors, including nitrate and oxygen (Myers & Nealson 1988).

Assimilatory ferric reductases are common to almost all aerobic bacteria, which must obtain iron under conditions where it is at low concentrations due to its spontaneous oxidation to insoluble ferric oxides. Many of these bacteria use high affinity iron-binding compounds called siderophores to scavenge the rare iron from the environment. Siderophore-Fe(III) complexes are then transported into the bacterial cells where the iron is reduced enzymatically and released from the siderophore. Enzymes with iron reductase activities have been detected in soluble fractions of *Escherichia*, *Pseudomonas* spp., and *Bacillus* spp., among others (Nealson & Saffarini 1994). Iron acquisition from hematite by an aerobic *Pseudomonas* sp. has also been demonstrated. In addition to the siderophore produced by the organism, heat stable, extracellular iron reductases were detected (Hersman et al. 1996).

Westlake and colleagues (Semple & Westlake 1987) reported isolation and characterization of a bacterium capable of dissimilatory iron reduction. This organism, originally identified as *Pseudomonas ferrireductans* and subsequently reclassified as *Shewanella putrefaciens* (McDonnell & Colwell 1985), was isolated from mine tailings and oilfield samples. *S. putrefaciens* can use an array of electron acceptors including oxygen, Fe(III), Mn(IV), NO_3^-, NO_2^-, $S_2O_3^{2-}$, SO_3^{2-}, fumarate, and others (Myers and Nealson 1988). The organism is unusual with regard to its capacity to use a range of carbon compounds, e.g., acetate is used aerobically but not anaerobically, and formate is used anaerobically but not aerobically. Most strains use lactate, pyruvate, and some amino acids under all conditions, while only a few strains use complex carbon sources such as glucose. In addition, *S. putrefaciens* can use hydrogen as an electron donor for reduction of metals (Nealson & Saffarini 1994).

Early reports of Obuekwe et al. (1981) suggested that iron-reducing bacteria play a role in corrosion of carbon steels. To investigate this possibility further, we designed experiments to monitor corrosion of carbon steel electrodes in the presence of wild-type *S. putrefaciens*. Synthetic iron oxides were used as model compounds for surface films on carbon steel surfaces. Microbial colonization and dissolution rates were determined. This paper represents an attempt to relate MIC to biomineralization of specific surface-bound iron oxides.

Materials and methods

Growth medium for metal reduction

S. putrefaciens was grown on the following medium: NaCl, 10 g; bacto-tryptone, 5 g; yeast extract, 2.0 g; HEPES buffer, 10 ml (1.0 M); 1.0 l distilled water. Synthetic iron oxides (goethite, ferrihydrite, and hematite) were prepared, characterized and added to 10 ml of growth medium that was then inoculated with 10^8 *S. putrefaciens* cells ml^{-1}. Minerals were examined directly using environmental scanning electron microscopy/energy dispersive x-ray spectroscopy (ESEM/EDS) and confocal laser scanning microscopy (CLSM).

ESEM/EDS sample preparation and instrument operation

Principles and operation of ESEM have been described elsewhere (Little et al. 1991b). Briefly, the ESEM (Electroscan Corp., Wilmington, MA) uses a secondary electron detector capable of forming high resolution images (50 È) at pressures in the range of 0.1 to 20 torr. At these relatively high pressures, specimen charging is dissipated into the gaseous environment of the specimen chamber, enabling direct observation of uncoated, nonconductive specimens. If water vapor is used as the specimen environment, wet samples can be observed. After 48, 72 and 190 h, two mL samples of the iron oxide minerals were extracted from anaerobic culture vials using an Eppendorf pipet, and dispensed into centrifuge tubes with 15 mL distilled water to remove residual culture medium from mineral surfaces before fixation. Suspensions were centrifuged for 2 min at a slow speed to precipitate solid particles, the supernatant decanted, and the rinse procedure repeated. One ml of sample with residual rinse water was extracted and fixed in 2% (v/v) glutaraldehyde buffered with sodium cacodylate (0.1 M, pH 7.2). Samples remained in the fixative for a minimum of 4 h, but usually overnight. Fixative was removed using the same rinsing procedure previously described. Five μl of the fixed, rinsed samples were extracted and placed directly into a counterbore type (0.1 cm $\times$ 0.04 cm deep) specimen mount of a Peltier cooling device in the ESEM chamber. Carbon steel electrodes were removed from the culture medium/electrolyte, fixed in 2% (v/v) glutaraldehyde buffered with sodium cacodylate and rinsed with two washes of distilled water. Wet coupons were placed directly on the Peltier cooling device in

the ESEM chamber. Samples were imaged at 20 keV with temperature (4°C) and chamber vapor pressure (4 torr) controlled so that condensation would keep samples moist. Elemental analysis of the samples was performed using EDS coupled to ESEM.

CLSM sample preparation and instrument operation

A full explanation of CLSM may be found elsewhere (Stelzer et al. 1991). Briefly, both illuminating light and light from the specimen are passed through the same optical path of a standard microscope, with the two paths being split at the ocular focal point. The specimen light is detected by a photomultiplier tube after passing through a 50–100 μm diameter pinhole. The pinhole eliminates out-of-focus portions of the image on the periphery of the light beam, i.e., light from above and below the image focal plane. The only light entering the detector is that which is in a very thin focal plane within the specimen. Because most light is discarded, a laser is used to provide sufficient intensity. The small laser spot is scanned in a raster pattern over the horizontal focal plane and the resulting analog signal is digitized in synchrony to produce images up to 1024 $\times$ 1024 pixels at a resolution of 0.05 μm per pixel and a vertical resolution of up to 0.1 μm. Although laser light can be used in most of the usual illumination modes of optical microscopy, it is most often used in CLSM as a fluorescence excitation source to increase specimen contrast in combination with specific fluorescent stains. A stepping motor is used to focus the microscope through the specimen at precise steps, and digital image reconstruction techniques are used to visualize the entire specimen volume, either as section planes of arbitrary orientation or as an extended focus image in which the entire specimen is in focus.

A 5 ml suspension of glutaraldehyde-fixed iron oxides was mixed with 5 ml of a proprietary fluorescent stain (LIVE/DEAD® *Bac*LIGHT^{TM}, Molecular Probes Inc., Eugene, OR) sealed under a 1-mm-thick coverslip for examination with a Sarastro 2000 confocal laser scanning microscope (Molecular Dynamics Corp., Sunnyvale, CA). This fluorescent stain is specific for microorganisms (i.e., mineral and most organic debris do not fluoresce), does not require rinsing before examination, and is resistant to photo bleaching. The stain distinguishes between viable cells (blue fluorescence) and nonviable cells (red fluorescence). Specimens were illuminated with the 488 nm line of an argon laser operated at 16 mW power. Images were captured at a horizontal resolution of 512 $\times$ 512 pixels at 0.1 mm each $\times$ 0.26 mm deep using a graphics workstation. A Kalman filter (an averaging algorithm) was used during image acquisition to improve resolution. Image acquisition, processing, volume modeling, and extended focus modeling were performed using ImageSpace® software (Molecular Dynamics). Color images were produced using a screen or video printer. The CLSM was operated at 488 nm in both the fluorescence and reflectance modes. Images were collected using a 100$\times$ oil immersion objective.

Metal oxide reduction experiments

Rates of mineral dissolution were monitored by measuring soluble Fe(II) using atomic absorption spectroscopy. Samples were filtered to remove solids (Fe(III)), and Fe(II) was quantified as a function of time.

Electrochemical corrosion experiments

Electrochemical noise analyses follow fluctuations of potential or current as a function of time or experimental conditions (Mansfeld & Little 1992). Analysis of the structure of electrochemical noise data using the frequency dependence of the power spectral density can provide information concerning the nature of the corrosion processes and magnitude of the corrosion rate. Electrochemical noise experiments were designed to demonstrate the importance of microbial iron reduction in MIC. Current noise vs. time experiments used a galvanic dual-cell controlled by a potentiostat (Wagner & Little 1986). UNS G10100 carbon steel electrodes were electronically coupled but biologically separated in two sterile half-cells. Precleaned and sterilized electrodes were exposed to sterile medium/electrolyte consisting of 7.5 ml HEPES (1.0 M) buffer, 0.75 g yeast extract, 2.0 g casamino acids, 7.5 ml sodium lactate (1.0 M, pH 7.33), and 15 ml sodium bicarbonate (0.2 M) solutions added to 1.5 l distilled water. In one experiment 30 g sodium chloride and 15 ml thiosulfate (1.0 M) were added to the medium/electrolyte. In a second experiment, sodium chloride and thiosulfate were removed from the medium/electrolyte so as to avoid corrosion due to chlorides and sulfides. After equilibration, one half-cell was inoculated with *S. putrefaciens* and the other half-cell was maintained abiotically. Nitrogen was bubbled into the half-cells throughout the duration of the experiment.

Table 1. Relative rates of iron reduction based on FE(II) in solution

	24 Hours mg/L/d	% Max	22 Days mg/L/d	% Max
Goethite	3.50	100	18.20	100
Ferrihydrite	2.60	74	14.10	77
Hematite	0.58	22	0.39	2

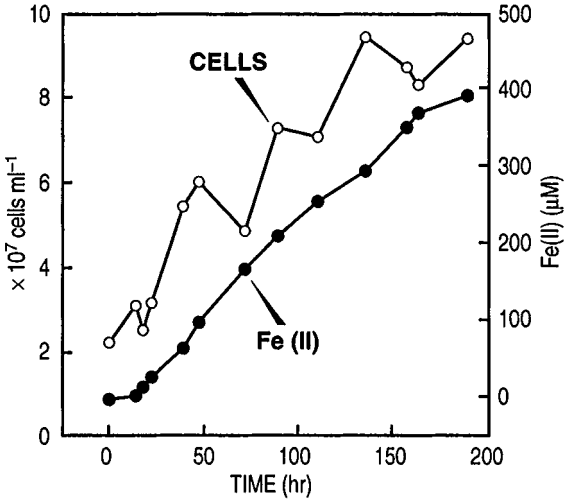

Figure 1. Bacterial reduction of goethite.

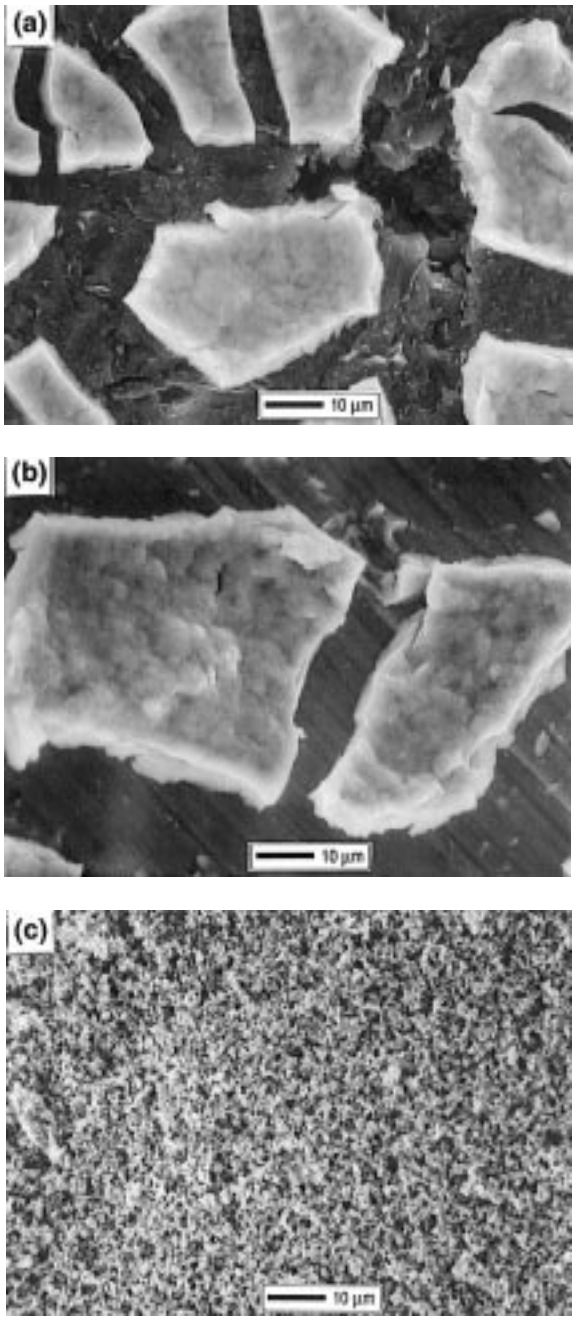

Figure 2. Iron oxides before exposure to *S. putrefaciens*: (a) goethite, (b) ferrihydrite, and (c) hematite.

Results and discussion

There is general agreement that oxide films formed on iron in air at temperatures below 200°C are composed of magnetite and hematite (Szklarska-Smialowska 1986). Szklarska-Smialowska (1986) described the formation of hematite over a magnetite film. Ferric oxyhydroxides, including goethite and lepidocrocite (γ-FeO·OH), have also been identified in oxide layers on carbon steel. During biomineralization, bacteria influence the kinetics of mineral dissolution; gain energy, enabling them to carry out respiration when oxygen is limiting or absent; and satisfy trace element requirements (Ehrlich 1996).

Under anaerobic conditions goethite, hematite, and ferrihydrite were reduced by *S. putrefaciens* (Table 1). Rates of reduction, indicated by atomic absorption spectroscopy measurements of Fe(II) in solution as a function of time, for the three minerals are different. Relative rates of iron reduction were normalized to the maximum reduction, in this experiment measured for goethite. After 24 h exposure to *S. putrefaciens*, initial reduction rates for goethite and ferrihydrite were approximately the same and were 5× faster than the reduction rate for hematite. After 22 days the integrated reduction rates for goethite and ferrihydrite were much faster than those measured at 24 h. The hematite reduc-

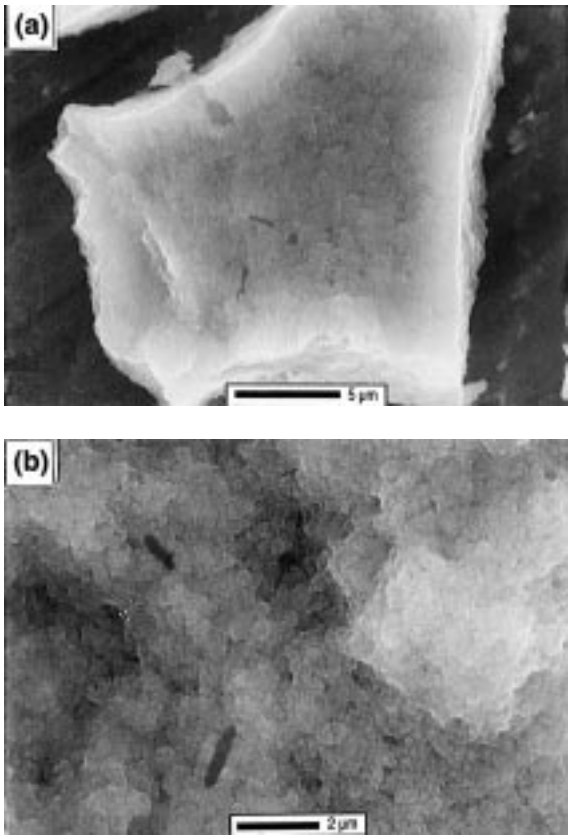

Figure 3. Bacteria on mineral surfaces after 48-h exposure to *S. putrefaciens*: (a) goethite and (b) ferrihydrite.

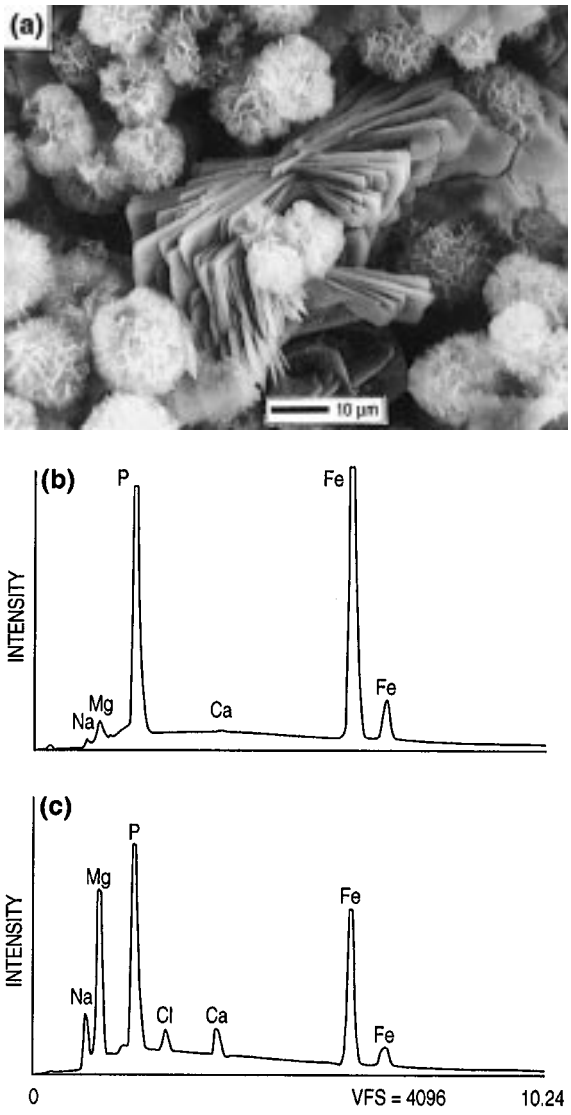

Figure 4. Goethite after 190-h exposure to *S. putrefaciens*: (a) ESEM image of particle, (b) EDS spectrum of crystalline plate forms, and (c) EDS spectrum of globular forms.

tion rate actually slowed over the exposure period so that after 22 days the overall integrated rate was 50× slower than reduction rates for goethite and ferrihydrite. Studies in this laboratory and elsewhere (Arnold et al. 1988) suggest that these differences can be due to the surface areas of the individual oxides. Mineralogy and crystal structure must also play a role, but these aspects have not been well investigated. Figure 1 shows the relationship between bacterial cell concentrations and Fe(II) in solution over time for goethite. Similarly, reduction studies with *Geobacter metallireducens* (Lovley & Woodward 1996) demonstrated that crystalline goethite was more readily reduced than crystalline hematite over a 4-h period. Rates of reduction were enhanced in the presence of nitrilotriacetic acid, an Fe(III) chelator.

Before exposure to *S. putrefaciens*, goethite and ferrihydrite appeared to form smooth platelet-like particles, while the hematite consisted of fine crystals (Figures 2a, 2b, and 2c). All iron oxides produced EDS spectra that were exclusively iron. After 48 h, isolated bacteria could be located on the surfaces of both the goethite and ferrihydrite (Figures 3a and 3b), but not on the hematite. Minerals viewed with ESEM were wet and not coated with a metal coating as required for standard scanning electron microscopy. During initial stages of mineral dissolution, bacteria composed of water and low atomic number elements were not electron dense and were difficult to image. With the reduction of the ferric iron, the bacterial cells became electron dense and easier to recognize. Fluorescence staining for CLSM images indicated that approximate-

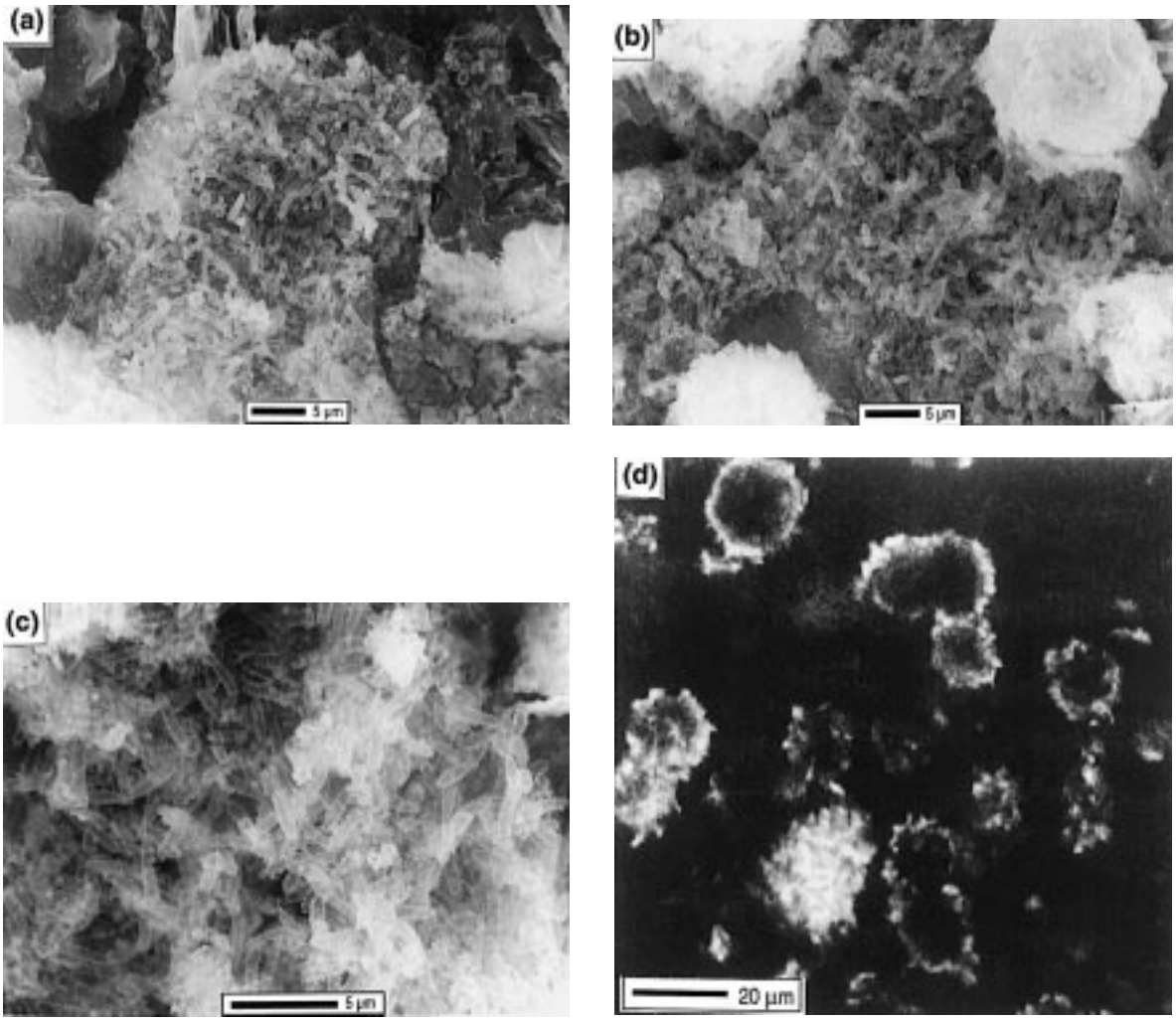

Figure 5. (a-c) Bacterial cells on goethite surface after 190-h exposure to *S. putrefaciens* and (d) CLSM image of optical cross-section of goethite particle.

ly 50% of all observed cells exhibited a blue fluorescence, indicating that they were probably viable. Occasionally dividing cells were observed. Surface microbial populations increased markedly after 72 h. Numerous studies (Myers & Nealson 1988) have suggested that Fe(III)-reducing microorganisms must be in direct contact with Fe(III) oxides to reduce them. This conclusion is based on the observation that Fe(III) is not reduced if microorganisms capable of Fe(III) reduction are separated from the Fe(III) oxides by a semipermeable membrane that allows exchange of soluble molecules but prevents contact between the organism and the oxide.

After 190 h, ESEM images demonstrated that goethite and ferrihydrite surfaces had been altered similarly during microbial reduction. Mineral particle size decreased and crystalline structure was transformed as the number of bacterial cells increased. Residual goethite particles consisted of both highly crystalline plates and more globular forms (Figure 4a). EDS spectra of the two newly formed structures showed that the crystalline plate forms consisted of nearly stoichiometric amounts of iron and phosphorus, with a small enrichment of magnesium, suggesting that this mineral might be iron phosphate (vivianite) (Figure 4b). Globular forms were chemically more complex, containing iron, phosphorous and magnesium (Figure 4c).

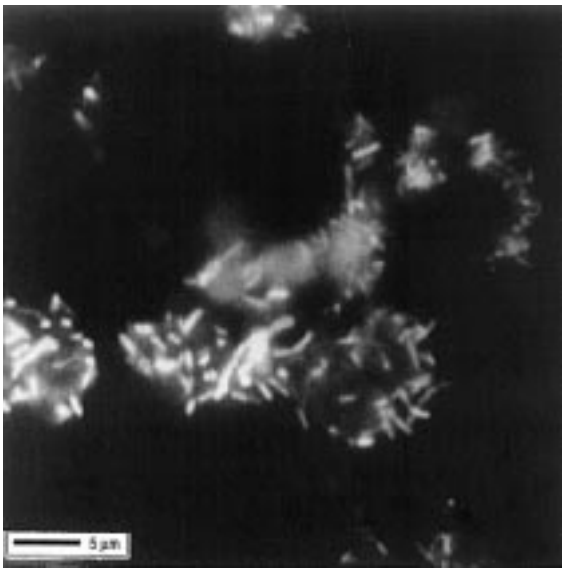

Figure 6. CLSM image of optical cross-section of ferrihydrite after 190-h exposure to *S. putrefaciens*.

The new mineral forms may represent iron carbonate (siderite), vivianite, or a mixed iron oxide such as magnetite (Fe_3O_4). In previous experiments iron oxides were converted to siderite and other carbonates when experiments were conducted in closed containers from which carbon dioxide could not escape. ESEM images of residual goethite particles documented large accumulations of cells (Figures 5a, 5b and 5c). The CLSM preparation of goethite particles contains a variety of sizes at different elevations within the preparation. The optical section in Figure 5d shows some particles that are completely covered with bright fluorescent cells. Other goethite particles have been optically cross-sectioned so that it is obvious that bacterial cells were associated with the exterior surfaces and had also created channels into the particles. ESEM images of ferrihydrite after 190 h had a similar appearance, but the CLSM images of optical sections indicated that individual particles could no longer be differentiated (Figure 6). Instead, bacterial cells were distributed throughout all optical depths. Although iron reduction of hematite occurred (Table 1), no major changes in the elemental composition or crystal structure of the surface (Figure 7a) were noted. The EDS spectrum of hematite indicated pure iron even after 190-h exposure. Scattered bacterial cells could be demonstrated in association with the surface of the dark hematite using CLSM (Figure 7b).

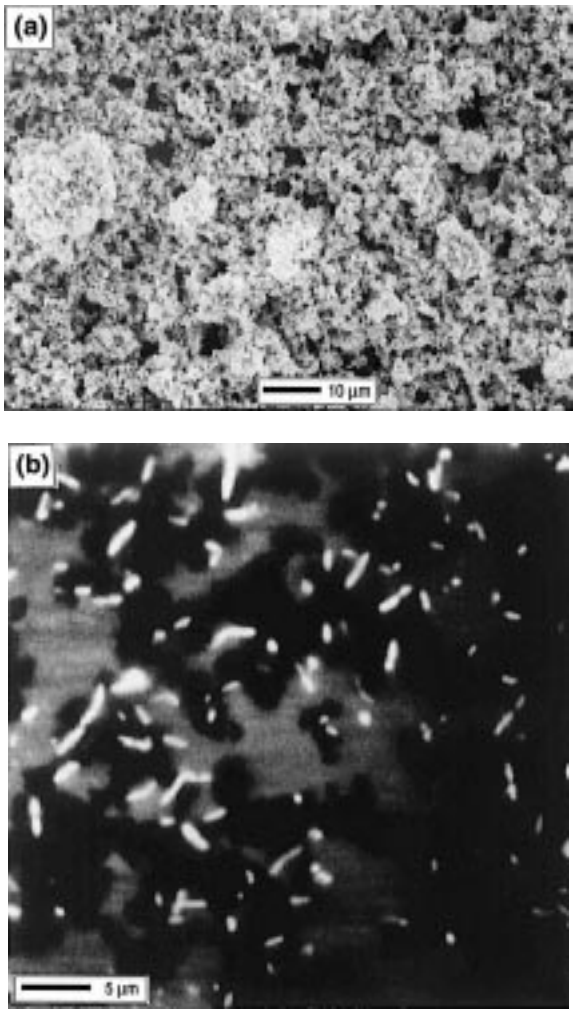

Figure 7. Hematite surface after 190-h exposure to *S. putrefaciens*: (a) ESEM image and (b) CLSM optical cross-section.

Current vs. time plots in media with and without the combination of sodium chloride and thiosulfate indicated substantial electrochemical noise (Figures 8a and 8b). In both cases the electrochemical noise showed active surface changes. Fluctuations in the noise record of a corroding metal are usually interpreted as being due to the sudden rupture of an oxide film followed by immediate reformation. As previously mentioned in the introduction, *S. putrefaciens* can reduce thiosulfate to produce sulfide. Obuekwe et al. (1981) evaluated corrosion of mild steel under conditions of simultaneous formation of ferrous and sulfide ions. They reported extensive pitting when both processes were active. When only sulfide was produced, initial corrosion rates increased but later declined due to formation of a pro-

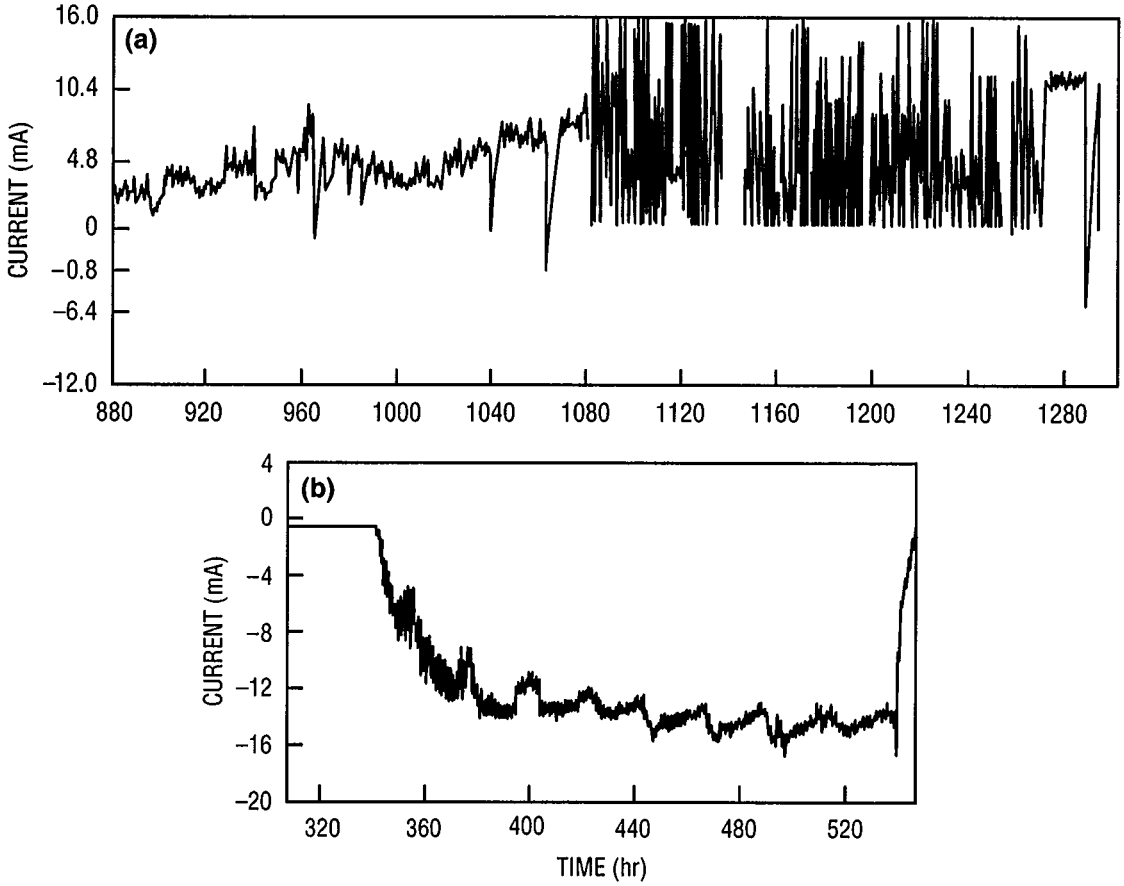

Figure 8. Plot of galvanic current vs. time for exposure of carbon steel to *S. putrefaciens* (a) in medium including thiosulfate and sodium chloride and (b) in medium without thiosulfate and sodium chloride.

tective FeS film. High concentrations of soluble iron prevent formation of protective sulfide layers on ferrous metals. In our experiments, attempts were made to isolate the impacts of iron and thiosulfate reduction on corrosion of carbon steel by controlling the electron acceptors available in the electrolyte. In the initial experiment, thiosulfate was added to the medium, while in the second it was removed. Substantial electrochemical noise was measured in both cases and both electrodes were pitted. Attempts are being made to convert the electrochemical noise to the frequency domain to determine more about the electrochemistry of carbon steel in the two media. In addition to manipulation of the medium to isolate the contributions of the two microbial processes, future experiments are being designed using mutants deficient in one or both of the iron and thiosulfate reductases.

ESEM examination of carbon steel electrodes revealed extensive bacterial colonization after 1300 h (Figure 9a). The electrode was macroscopically pitted, and the location of pits coincided with colonies of bacteria (Figure 9b). EDS analysis of the electrode surface showed that, like goethite and ferrihydrite, the modified surface, while still iron rich, had a complex mixture of elements, including phosphorous, sulfur, and chlorine (Figure 9c).

Chemical, visual, and electrochemical data are consistent with induction of corrosion by the metal-reducing bacteria. Metal reduction is coupled to anaerobic oxidation of organic carbon. The possibility exists that biomineralization is closely tied to corrosion, and that dissimilatory iron and/or manganese reducers represent one of the important components of the complex community responsible for corrosion.

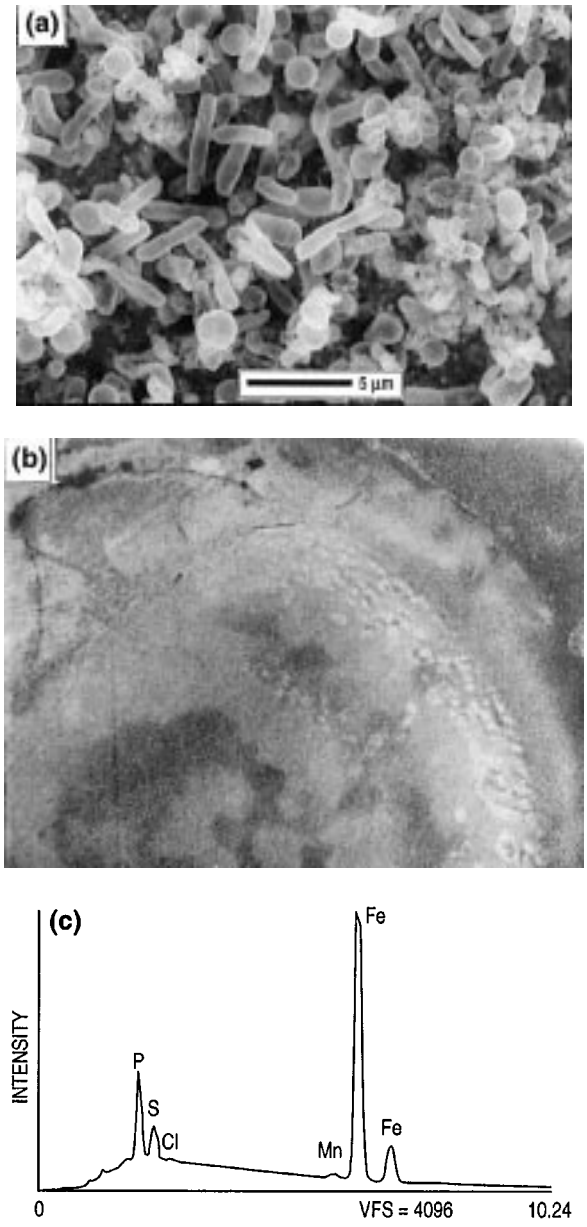

Figure 9. Carbon steel electrode after 1300-h exposure to *S. putrefaciens*: (a) bacterial colonization, (b) surface pitting (12×), and (c) EDS of surface.

Conclusions

Microorganisms influence corrosion by both forming and dissolving minerals. Biomineral dissolution reactions by metal-reducing bacteria, as discussed in this paper, remove oxide layers or force mineral replacement reactions that lead to further dissolution of metal. Biomineralization that results in mineral deposition on a metal surface can shift the corrosion potential in either a positive or negative direction, depending on the nature of the mineral. For example, manganese oxide biodeposition on stainless steel surfaces forces a shift in the positive, more noble direction, moving the corrosion potential toward the pitting potential and making some metals more vulnerable to pitting and crevice corrosion. Bioprecipitated sulfides move the corrosion potential in a negative, more active direction, resulting in accelerated corrosion of some metals and alloys. Iron oxide formation can initiate a sequence of events that results in underdeposit corrosion of susceptible metals.

Acknowledgments

This work was performed under Program Element 0601153N, NRL Contribution Number NRL/JA/7333–96-0035, Office of Naval Research Contract No. N001497WX30031.

References

American Petroleum Institute (1965) API recommended practice for biological analysis of subsurface injection waters, NY, NY

Arnold RG, DiChristina T & Hoffmann M (1988) Reductive dissolution of Fe(III) oxides by *Pseudomonas* sp. 200. Biotechnol. Bioeng. 32: 1081–1096

Boivin J, Laishley EJ, Bryant RD & Costerton JW (1990) The influence of enzyme systems on MIC, CORROSION/90, paper no. 128, NACE International, Houston, TX

Ehrlich HL (1996) How microbes influence mineral growth and dissolution. Chem. Geol. 132: 5–9

Hersman L, Maurice P & Sposito G (1996) Iron acquisition from hydrous Fe(III)-oxides by an aerobic *Pseudomonas* sp.. Chem. Geol. 132: 25–31

Little B, Wagner P & Mansfeld F (1991a) Microbiologically influenced corrosion of metals and alloys. Int. Mat. Rev. 36, 6: 253–272

Little B, Wagner P, Ray R, Pope R & Scheetz R (1991b) Biofilms: an ESEM evaluation of artifacts introduced during SEM preparation. J. Industr. Microbiol. 8: 213–222

Lovley DR & Woodward JC (1996) Mechanisms for chelator stimulation of microbial Fe(III)-oxide reduction. Chem. Geol. 132: 19–24

Mansfeld F & Little B (1992) Electrochemical techniques applied to studies of microbiologically influenced corrosion (MIC). Trends in Electrochemistry 1: 47–61

McDonnell MT & Colwell RR (1985) Phylogeny of the Vibrionaceae, and recommendation for two new genera, *Listonella* and *Shewanella*. Syst. Appl. Microbiol. 6: 171–182

McNeil MB, Jones JM & Little BJ (1991) Mineralogical fingerprints for corrosion processes induced by sulfate-reducing bacteria. CORROSION/91, paper no. 580, NACE International, Houston, TX

McNeil MB & Little BJ (1990) Mackinawite formation during microbial corrosion. Corrosion 46 (7): 599–600

Myers C & Nealson K (1988) Bacterial manganese reduction and growth with manganese oxide as the sole electron acceptor. Science 240: 1319–1321

Nealson KH & Saffarini DA (1994) Iron and manganese in anaerobic respiration. Ann. Rev. Microbiol. 48: 311–343

Obuekwe CO, Westlake DWS, Plambeck JA & Cook FD (1981) Corrosion of mild steel in cultures of ferric iron reducing bacterium isolated from crude oil I. polarization characteristics. Corrosion 37, 8: 461–467

Pope DH, Duquette DJ, Wayner Jr. PC & Johannes AH (1984) Microbiologically influenced corrosion: a state of the art review, Materials Technology Institute of the Chemical Process Industries, Columbus, OH

Semple K & Westlake D (1987) Characterization of iron-reducing *Alteromonas putrefaciens* strains from oil field fluids. Can. J. Microbiol. 33: 366–371

Stelzer EHK, Wacker I & DeMey JR (1991) Confocal fluorescence microscopy in modern cell biology. Cell Biology 2: 145–152

Szklarska-Smialowska Z (1986) Pitting Corrosion of Metals. NACE International, Houston, TX

Tatnall RE, Stanton KM & Ebersole RC (1988) Methods of testing for the presence of sulfate-reducing bacteria, CORROSION/88, paper no. 88, NACE International, Houston, TX

Wagner P & Little B (1986) Applications of a technique for the investigation of microbially induced corrosion. CORROSION/86, paper no. 121, NACE International, Houston, TX